Array-aided single-differenced satellite phase bias determination: methodology and results

Amir Khodabandeh
GNSS Research Centre, Department of Spatial Sciences
Curtin University of Technology, Perth, Australia

BIOGRAPHY

Amir Khodabandeh received the MSc degree in Geodesy from University of Tehran, Iran, in 2011. He is currently pursuing the PhD degree at the GNSS Research Centre, Curtin University of Technology. His research interests comprise estimation theory, GNSS precise positioning and GNSS quality control.

ABSTRACT

Integer ambiguity resolution at a single GNSS receiver gets feasible, if network-derived satellite phase biases (SPBs), among other corrections, are a-priori available. In this paper, the concept of array-aided between-satellite single-differenced (SD) SPB determination is introduced which is aimed to reduce the code-dominated precision of SD-SPB corrections. The underlying model is realized by giving the role of the local reference network to an array of antennas, mounted on rigid platforms, that are separated by a few meters only. A closed-form expression of the array-aided SD-SPB corrections is presented, thereby proposing a simple strategy to compute the SD-SPBs. Upon resolving double-differenced ambiguities of the array's data, the variance of the SD-SPB corrections is shown to be reduced by a factor equal to the number of antennas. This improvement in precision is also affirmed by numerical results. Experimental results demonstrate that the user's integer-recovered ambiguities converge to integers faster, upon increasing the number of antennas aiding the SD-SPB corrections. Integrated with the ionospheric corrections, the stated SD-SPB corrections carry over the precision improvement to the user's position as well.

INTRODUCTION

Employing GNSS network-derived orbit/clock corrections, single-station precise point positioning (PPP) has proved to be an efficient technique [1, 2]. Biased by the real-valued (but time-constant) estimable ambiguities, the very precise phase observables would, however, not take a truly active part in estimating the user's position, unless a rather long convergence time takes place—longer than 30 min to attain sub-decimeter level of accuracy [3, 4]. Fast and centimeter level PPP would therefore get feasible, if the ambiguities are successfully resolved to integer values. Unfortunately, because of the presence of the satellite hardware biases in the phase and code data, the estimable between-satellite single-differenced (SD) ambiguities of the PPP user are not of an integer nature. In other words, the integer-valued ambiguities cannot be separated from these biases.

Recent contributions have demonstrated that the stated satellite hardware biases can be properly defined and estimated as the estimable satellite phase biases (also referred to as uncalibrated phase delays or fractional cycle biases), see e.g. [5–13]. Among which, reliable determination of the satellite phase biases (SPBs), on the basis of a local network of reference stations, is also acknowledged [14–16]. Given a-priori network-derived SPBs, the integer property of the user's SD ambiguities is thus recovered, giving rise to single-station integer ambiguity resolution. In this respect, the estimable SPBs are either presented in their undifferenced non-combined form [10, 14, 16], undifferenced combined form [15, 17], between-satellite SD non-combined form [18], between-satellite SD combined form [6, 12], or assimilated into the clocks defining decoupled phase clock parameters [7, 8, 13].

As shown in the contributions by [16, 18], the precision of the non-combined SPB corrections is governed by the code noise. Although significantly shortening the convergence time, PPP ambiguity resolution does therefore still take about 15 min of time to reliably fix the ambiguities to their integers, would no ionospheric corrections be applied [19]. Since a high code-dominated correlation between the SPB corrections and the ionospheric corrections exists, the noise of the code data is, however, canceled out when these two types of corrections are com-

bined to correct the user's phase data. The precision of the user's phase correction is then governed by the phase noise, thereby providing outcomes comparable to the network real-time kinematic solutions [18].

In this paper, the concept of array-aided between-satellite SD-SPB determination is introduced. We convey the idea of SPB determination to the case where the role of the local reference network is taken by an array of antennas, mounted on rigid platforms, that are separated by a few meters only [20, 21]. The objective of this study is twofold. First, an efficient strategy is sought to reduce the code-dominated noise of the SD-SPB corrections, expediting the convergence of the user's integer-recovered ambiguities over time. Second, the user's position improvement is aimed to be realized, once the array-aided SD-SPB corrections are combined with their ionospheric counterparts. We commence with a closed-form analytical expression of the SD-SPB corrections using one single antenna. The contribution of the aiding antennas to the precision of the SD-SPB corrections is then formulated. Upon resolving double-differenced (DD) ambiguities, the code-dominated variance of the SD-SPB corrections is shown to be reduced by a factor equal to the number of antennas. Thus the larger the number of antennas are utilized, the more precise the array-aided SD-SPB corrections become. Presenting a closed-form expression of the array-aided SD-SPB corrections, a simple algorithm to compute them is outlined afterwards. The performance of the proposed methodology is validated by a GPS campaign collecting dual-frequency data.

FULL-RANK MODEL

Consider a reference antenna, say $r = 1$, tracking dual-frequency GNSS data that are transmitted by satellite s and a chosen pivot satellite p. The corresponding between-satellite SD observation equations read then [22]

$$\begin{aligned} \mathsf{E}\{\underline{\phi}^{ps}_{1,j}\} &= \rho^{ps}_1 - \mu_j \iota^{ps}_1 + \lambda_j (a^{ps}_{1,j} - \delta^{ps}_{,j}) \\ \mathsf{E}\{\underline{p}^{ps}_{1,j}\} &= \rho^{ps}_1 + \mu_j \iota^{ps}_1 - d^{ps}_{,j} \end{aligned} \tag{1}$$

where $\underline{\phi}^{ps}_{1,j}$ and $\underline{p}^{ps}_{1,j}$ denote the between-satellite SD phase and code observables on the frequency band f_j ($j = 1,2$), respectively. The non-dispersive parameter ρ^{ps}_1 captures the SD geometric ranges, SD tropospheric delays, as well as the SD satellite clock parameters. The (first-order) SD slant ionospheric delay, experienced on the first frequency, is denoted by ι^{ps}_1. Thus the frequency-dependent coefficients are defined as the ratio $\mu_j = (f_1^2/f_j^2)$. Expressed in cycles, the SD ambiguity is composed of the integer-valued parameter $a^{ps}_{1,j}$ and the SD-SPB $\delta^{ps}_{,j}$ which are linked to the phase observables through the wavelength λ_j. Likewise, the SD satellite code hardware delays are denoted by $d^{ps}_{,j}$. Random variables are indicated by an underscore ($\underline{.}$), and $\mathsf{E}\{.\}$ denotes the expectation operator. We remark, apart from $a^{ps}_{1,j}$ and $\delta^{ps}_{,j}$, that the rest of the quantities have been expressed in units of range.

The observation equations, given in (1), do not represent a full-rank model, in the sense that the parameters involved cannot be separated from one another. It is therefore only possible to estimate combinations of the parameters. These estimable combinations are formed according to the minimum set of parameters which need to be lumped with the remaining parameters so that the underlying rank-deficiency is eliminated [9]. This minimum set of parameters is referred to as an $\mathcal{S}$-basis of the model defining a minimum number of constraints through which the model becomes of full-rank [23, 24].

As shown in [16, 18], the code hardware delays $d^{ps}_{,j}$ and the integer-valued ambiguities $a^{ps}_{1,j}$ can, for instance, be chosen as the $\mathcal{S}$-basis of the model. In doing so, we define the ionosphere-free (IF) and geometry-free (GF) combinations of $d^{ps}_{,j}$ ($j = 1,2$), respectively, as

$$\begin{aligned} d^{ps}_{,IF} &= \tfrac{\mu_2}{\mu_{12}} d^{ps}_{,1} - \tfrac{\mu_1}{\mu_{12}} d^{ps}_{,2}, \\ d^{ps}_{,GF} &= -\tfrac{1}{\mu_{12}} d^{ps}_{,1} + \tfrac{1}{\mu_{12}} d^{ps}_{,2}, \quad \text{with} \quad \mu_{12} = \mu_2 - \mu_1 \end{aligned} \tag{2}$$

On the basis of the above definition, the original code hardware delays stand in *one-to-one* correspondence with their IF and GF counterparts through

$$d^{ps}_{,j} = d^{ps}_{,IF} + \mu_j d^{ps}_{,GF}, \quad j = 1,2 \tag{3}$$

Clearly, the IF component $d^{ps}_{,IF}$ is absorbed by the non-dispersive parameter ρ^{ps}_1, while the GF component $d^{ps}_{,GF}$ is absorbed by the ionospheric delay ι^{ps}_1. This yields the following estimable combinations

$$\tilde{\rho}^{ps}_1 = \rho^{ps}_1 - d^{ps}_{,IF}, \qquad \tilde{\iota}^{ps}_1 = \iota^{ps}_1 - d^{ps}_{,GF} \tag{4}$$

Substituting $\rho^{ps}_1 = \tilde{\rho}^{ps}_1 + d^{ps}_{,IF}$ and $\iota^{ps}_1 = \tilde{\iota}^{ps}_1 + d^{ps}_{,GF}$ into (1), a full-rank model is then structured by lumping $a^{ps}_{1,j}$ with $\delta^{ps}_{,j}$, that is

$$\begin{aligned} \mathsf{E}\{\underline{\phi}^{ps}_{1,j}\} &= \tilde{\rho}^{ps}_1 - \mu_j \tilde{\iota}^{ps}_1 - \lambda_j \tilde{\delta}^{ps}_{,j} \\ \mathsf{E}\{\underline{p}^{ps}_{1,j}\} &= \tilde{\rho}^{ps}_1 + \mu_j \tilde{\iota}^{ps}_1, \end{aligned} \tag{5}$$

where the estimable SD-SPBs take the following form

$$\boxed{\tilde{\delta}^{ps}_{,j} = \delta^{ps}_{,j} - \tfrac{1}{\lambda_j} d^{ps}_{,IF} + \tfrac{\mu_j}{\lambda_j} d^{ps}_{,GF} - a^{ps}_{1,j}} \tag{6}$$

Therefore, the estimable SD-SPBs are composed of the *true* SD-SPBs, the SD satellite code hardware delays and

the SD ambiguities of the reference antenna. When expressed in units of range rather than in cycles, the above estimable SD-SPBs become indeed identical to those presented in [18].

METHODOLOGY

Single-antenna SD-SPB corrections

The number of observations in (5) is as many as the number of estimable parameters. In particular, the number of $\tilde{\delta}^{ps}_{,j}$ is equal to that of $\underline{\phi}^{ps}_{1,j}$ and, at the same time, the estimable SD-SPBs are not present in the code observables. The phase observables are thus fully reserved to determine the estimable SD-SPBs. As a consequence, the estimable parameters $\tilde{\rho}^{ps}_1$ and $\tilde{\imath}^{ps}_1$ are, respectively, determined by the IF and GF combinations of the code observables only, i.e.

$$\begin{aligned} \hat{\underline{\rho}}^{ps}_1 &= \underline{p}^{ps}_{1,IF} = \tfrac{\mu_2}{\mu_{12}}\underline{p}^{ps}_{1,1} - \tfrac{\mu_1}{\mu_{12}}\underline{p}^{ps}_{1,2}, \\ \hat{\underline{\imath}}^{ps}_1 &= \underline{p}^{ps}_{1,GF} = -\tfrac{1}{\mu_{12}}\underline{p}^{ps}_{1,1} + \tfrac{1}{\mu_{12}}\underline{p}^{ps}_{1,2}, \end{aligned} \tag{7}$$

with notation $\hat{}$ indicating the estimator of the quantities. Given the above code-based estimators, the single-antenna estimator of the estimable SD-SPBs follows from the first expression of (5), namely

$$\boxed{\hat{\underline{\tilde{\delta}}}^{ps}_{,j} = \tfrac{1}{\lambda_j}(\underline{p}^{ps}_{1,IF} - \mu_j \underline{p}^{ps}_{1,GF} - \underline{\phi}^{ps}_{1,j})} \tag{8}$$

Thus, in addition to the phase observables, the single-antenna SD-SPB estimator is a linear function of the IF and GF code combinations as well.

From single-epoch estimator to multi-epoch estimator

The estimator, given in (8), is based on data of one single epoch, i.e. the SD-SPBs are assumed to be unlinked in time. It is therefore referred to as the single-epoch estimator. In cases where information on the temporal behavior of the parameters, in (1), are assumed given, a joint estimation procedure of the estimable parameters, over time, must be applied [10]. In this study, we only assume the SD-SPBs, the SD satellite code hardware delays, along with the SD ambiguities to behave constant over time. The rest of the parameters are considered to be unlinked in time. Upon these assumptions, the multi-epoch estimator of the estimable SD-SPBs follows by weighted averaging its single-epoch counterparts over epochs, that is

$$\hat{\underline{\tilde{\delta}}}^{ps}_{,j}[k] = \frac{1}{\sum_{i=1}^{k} w_i^{ps}} \sum_{i=1}^{k} w_i^{ps}\, \hat{\underline{\tilde{\delta}}}^{ps}_{,j}(i) \tag{9}$$

where $\hat{\underline{\tilde{\delta}}}^{ps}_{,j}[k]$ denotes the multi-epoch estimator of the SD-SPBs over k epochs. The single-epoch estimator of the

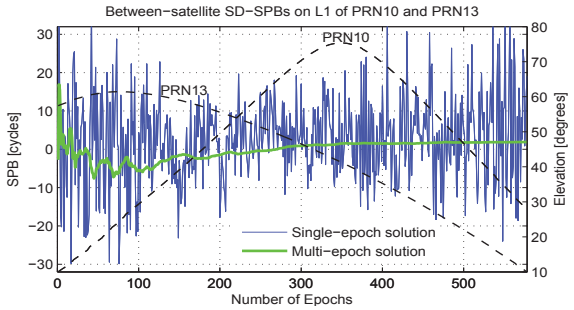

Figure 1. Single-epoch SD-SPB corrections (in blue) compared to its multi-epoch counterparts (in green) over time. Satellites' elevation is depicted in black dashed line.

SD-SPBs, based on the data of epoch i, is denoted by $\hat{\underline{\tilde{\delta}}}^{ps}_{,j}(i)$. The nonnegative weights w_i^{ps} $(i = 1,\ldots,k)$ capture the dependency of the GNSS data on the satellites' elevation. Here we make use of the exponential elevation weighting strategy [25]. They are, namely, computed as

$$w_i^{ps} = (\frac{1}{w_i^p} + \frac{1}{w_i^s})^{-1}, \tag{10}$$

with

$$w_i^q = [1 + 10\exp(-\frac{\varepsilon_i^q}{10^\circ})]^{-2}, \quad q = p,s \tag{11}$$

where ε_i^q is the elevation of satellite q [degree] at epoch i with respect to the reference antenna.

Fig. 1 shows typical examples of the single-epoch and multi-epoch versions of the SD-SPB corrections. It is observed that the size of the fluctuations of the single-epoch corrections increases as the elevation of the satellites decreases, showing the elevation dependency of the SD-SPB corrections. As the number of epochs increases, the multi-epoch SD-SPB corrections get more stable in time and converge to a constant value.

From non-combined SD-SPBs to combined SD-SPBs

The closed-form expression of (8) enables us to analyze the precision of the single-epoch single-antenna SD-SPB estimator. Consider GPS dual-frequency data where the code observables on both the frequencies are assumed to be uncorrelated and equally precise. Uncorrelated with the code data, the phase observables are also assumed to be uncorrelated and equally precise. Let σ_p and $\sigma_\phi = 0.01\sigma_p$ be the standard deviations of the between-satellite SD code and phase observables *in meters*, respectively. Then an application of the error propagation law to (8) gives

$$\sigma_{\hat{\tilde{\delta}}^{ps}_{,L1}} \approx 26.95\,\sigma_p\ [cycle], \quad \sigma_{\hat{\tilde{\delta}}^{ps}_{,L2}} \approx 26.75\,\sigma_p\ [cycle] \tag{12}$$

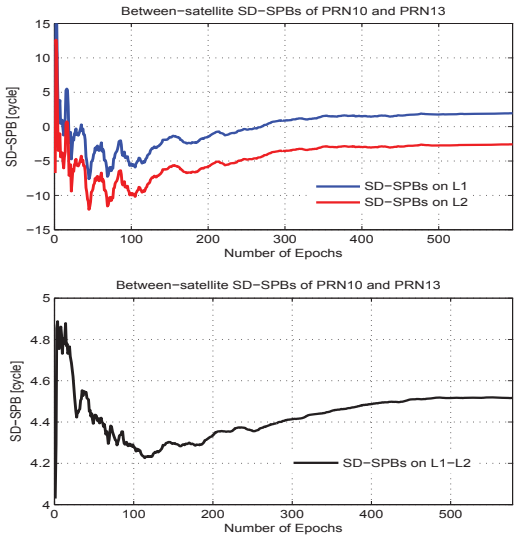

Figure 2. *Top-panel*: Multi-epoch SD-SPB corrections on L1 (in blue) and on L2 (in red). *Bottom-panel*: Multi-epoch SD-SPB corrections on L1-L2, i.e. wide-lane SD-SPB corrections (in black).

with $\sigma_{\check{\delta}^{ps}_{,L1}}$ and $\sigma_{\check{\delta}^{ps}_{,L2}}$ being, respectively, the standard deviations of the SD-SPBs on L1 and L2. Thus the precision of the non-combined SD-SPBs is heavily dominated by the noise of the code data. The error propagation law also provides us with the *cross-correlation* between the SD-SPBs on L1 and L2. The stated correlation is about 0.9996 which is indeed very significant. As shown in Fig. 2 (top-panel), the signatures of the SD-SPB corrections on both the frequencies are almost the same, corroborating that the SD-SPBs on L1 and L2 are highly correlated.

Of the combined SD-SPBs, we consider the wide-lane SD-SPBs that are defined as the between-frequency difference of the non-combined SD-SPBs (i.e. those on L1-L2). Given the standard deviations of the non-combined SD-SPBs (cf. (12)), together with their cross-correlation, the standard deviation of $\underline{\check{\delta}}^{ps}_{,L1-L2} = \underline{\check{\delta}}^{ps}_{,L1} - \underline{\check{\delta}}^{ps}_{,L2}$ is obtained as

$$\sigma_{\check{\delta}^{ps}_{,L1-L2}} \approx 0.83\,\sigma_p \;[cycle] \tag{13}$$

which is about 32 times smaller than those of the SD-SPBs on L1 and L2. The correlation between the SD-SPBs on L1 and L1-L2 is about 0.2581. As shown in Fig. 2 (bottom-panel), the size of the variations of the SD-SPB corrections on L1-L2 is much smaller than that of their non-combined counterparts, while their signature is quite different from that of L1 and L2. In order to appreciate the high correlation between SD-SPBs on L1 and L2, we therefore present those corresponding to L1 and L1-L2 in our further numerical results.

Array-aided SD-SPB corrections

To reduce the code-dominated noise of the SD-SPB corrections (cf. (12)), one may think of including the data of another antenna, say r ($r \neq 1$), for which a similar full-rank model can be formed by replacing subscript 1 with r in (5). As shown in (6), our earlier estimable SD-SPBs depend on the ambiguities of the reference antenna $a^{ps}_{1,j}$. The new full-rank model would, however, offer another form of the estimable SD-SPBs dependent on $a^{ps}_{r,j}$ instead, that is

$$\tilde{\check{\delta}}^{ps}_{,j} = \delta^{ps}_{,j} - \frac{1}{\lambda_j} d^{ps}_{,IF} + \frac{\mu_j}{\lambda_j} d^{ps}_{,GF} - a^{ps}_{r,j} \tag{14}$$

where their corresponding estimator reads (cf. (8))

$$\underline{\tilde{\check{\delta}}}^{ps}_{,j} = \frac{1}{\lambda_j}(\underline{p}^{ps}_{r,IF} - \mu_j \underline{p}^{ps}_{r,GF} - \underline{\phi}^{ps}_{r,j}) \tag{15}$$

Comparing (14) with (6), these new estimable SD-SPBs are related to $\tilde{\delta}^{ps}_{,j}$ through

$$\tilde{\check{\delta}}^{ps}_{,j} = \tilde{\delta}^{ps}_{,j} - a^{ps}_{1r,j}, \tag{16}$$

with the DD ambiguities $a^{ps}_{1r,j} = a^{ps}_{r,j} - a^{ps}_{1,j}$.

According to (16), including the data of antenna r results in two additional equations $\underline{\tilde{\check{\delta}}}^{ps}_{,j}$ ($j = 1,2$), given in (15), at the expense of two *unknown* DD ambiguities $a^{ps}_{1r,j}$ ($j = 1,2$). Therefore, as long as the DD ambiguities are unresolved, the extra antenna r has no contribution to the determination of the SD-SPBs $\tilde{\delta}^{ps}_{,j}$.

Let us, for the moment, assume $a^{ps}_{1r,j}$ to be successfully fixed to their integers $\breve{a}^{ps}_{1r,j}$. With (8) and (15), we then arrive at the following equations

$$\begin{aligned} \mathsf{E}\{\underline{\tilde{\check{\delta}}}^{ps}_{,j}\} &= \tilde{\delta}^{ps}_{,j} \\ \mathsf{E}\{\underline{\tilde{\check{\delta}}}^{ps}_{,j}\} + \breve{a}^{ps}_{1r,j} &= \tilde{\delta}^{ps}_{,j} \end{aligned} \tag{17}$$

in which the first expression characterizes the contribution of the reference antenna $r = 1$, while the second expression characterizes that of the extra antenna $r \neq 1$. Assuming the receivers/antennas of the *same* type, one can simply consider the average of the above two sets of equations as the improved estimator of the SD-SPB corrections $\tilde{\delta}^{ps}_{,j}$. The idea can be generalized to the case where the data of $n-1$ extra antennas $r = 2,\ldots,n$ are incorporated into the model. Given the resolved DD ambiguities, the array-aided SD-SPB estimator $\underline{\tilde{\check{\delta}}}^{ps}_{,j}$ reads then

$$\boxed{\underline{\tilde{\check{\delta}}}^{ps}_{,j} = \tfrac{1}{\lambda_j}(\underline{p}^{ps}_{\bar{r},IF} - \mu_j \underline{p}^{ps}_{\bar{r},GF} - \underline{\phi}^{ps}_{\bar{r},j}) + \breve{a}^{ps}_{1\bar{r},j}} \tag{18}$$

Table 1. Information on the location/type/data of the receivers/antennas, date and sampling interval as used in the experiment.

	User data-set	Array data-set
Location:	Curtin Uni. (Lat: 32.01° S, Long: 115.89° E)	South Perth (Lat: 31.98° S, Long: 115.86° E)
Type of receiver/antenna:	Javad TRE_G3T Delta/Javad Grant G3	Javad TRE_G3T Delta/Javad Grant G3
Number of antennas:	1	4
Data:	GPS dual-frequency (C/A, P2, L1, L2)	GPS dual-frequency (C/A, P2, L1, L2)
Date and time:	12 September, 2013 (00:00:00-11:32:00 GPST)	12 September, 2013 (00:00:00-11:32:00 GPST)
Sampling interval:	30 seconds	30 seconds

in which the following quantities are introduced

$$\begin{aligned} \underline{p}^{ps}_{\bar{r},IF} &= \tfrac{1}{n}\sum_{r=1}^{n}\underline{p}^{ps}_{r,IF}, \qquad \underline{p}^{ps}_{\bar{r},GF} = \tfrac{1}{n}\sum_{r=1}^{n}\underline{p}^{ps}_{r,GF} \\ \underline{\phi}^{ps}_{\bar{r},j} &= \tfrac{1}{n}\sum_{r=1}^{n}\underline{\phi}^{ps}_{r,j}, \qquad \breve{a}^{ps}_{1\bar{r},j} = \tfrac{1}{n}\sum_{r=1}^{n}\breve{a}^{ps}_{1r,j} \end{aligned} \tag{19}$$

with $\breve{a}^{ps}_{11,j} = 0$.

Since the array-aided SD-SPB estimator $\underline{\breve{\delta}}^{ps}_{,j}$ is structured by the average of the data of n antennas, its variance is n times smaller than that of the single-antenna estimator $\underline{\hat{\delta}}^{ps}_{,j}$, provided that the data of all the antennas are equally precise. Thus their standard deviations are related to one another through

$$\sigma_{\underline{\breve{\delta}}^{ps}_{,j}} = \frac{1}{\sqrt{n}}\,\sigma_{\underline{\hat{\delta}}^{ps}_{,j}} \tag{20}$$

Array-based ambiguity-fixing

As stated before, the data of the extra antennas do not contribute to the determination of the SD-SPBs, would the DD ambiguities remain unresolved. This is why one needs the average of the resolved ambiguities $\breve{a}^{ps}_{1r,j}$ $(r = 1,\ldots,n)$ to form the array-aided SD-SPB estimator in (18).

Although GNSS ambiguity-fixing is generally a bit involved, the procedure gets, however, considerably easier if simplified assumptions are placed on the model. Here, we consider an array of antennas separated by a few meters only. In this case, almost the same ionospheric delays are experienced by the antennas, that is $\iota^{ps}_{1r} = \iota^{ps}_{r} - \iota^{ps}_{1} \approx 0$ $(r = 2,\ldots,n)$. Given information on the geometry of the satellites/antennas, the DD geometric ranges are computed, namely $\underline{\hat{\rho}}_{1r} = \underline{\hat{\rho}}_{r} - \underline{\hat{\rho}}_{1}$ $(r = 2,\ldots,n)$. The float DD ambiguities are then obtained as follows

$$\underline{\hat{a}}^{ps}_{1r,j} = \frac{1}{\lambda_j}(\underline{\phi}^{ps}_{1r,j} - \underline{\hat{\rho}}^{ps}_{1r}), \quad r = 2,\ldots,n \tag{21}$$

with $\underline{\hat{a}}^{ps}_{1r,j}$ and $\underline{\phi}^{ps}_{1r,j} = \underline{\phi}^{ps}_{r,j} - \underline{\phi}^{ps}_{1,j}$ being the DD float ambiguities and phase observables, respectively. Having successfully resolved the DD float ambiguities, the algorithmic steps in computing the array-aided SD-SPB corrections have been summarized in Fig. 3.

Input
- SD GNSS data: $\underline{\phi}^{ps}_{r,j}$, $\underline{p}^{ps}_{r,j}$ for $r = 1,\ldots,n$; $j = 1,2$
- DD geometric ranges ρ^{ps}_{1r} for $r = 2,\ldots,n$
- coefficients λ_j and μ_j for $j = 1,2$

Begin
- Form the IF and GF combinations $\underline{p}^{ps}_{r,IF}$ and $\underline{p}^{ps}_{r,GF}$ for $r = 1,\ldots,n$ (cf. (7))
- Compute the float ambiguities $\underline{\hat{a}}^{ps}_{1r,j}$ for $r = 2,\ldots,n$; $j = 1,2$ (cf. (21))
- Resolve $a^{ps}_{1r,j}$ and obtain $\breve{a}^{ps}_{1r,j}$ for $r = 1,\ldots,n$; $j = 1,2$, with $\breve{a}^{ps}_{11,j} = 0$
- Compute the averages $\underline{\phi}^{ps}_{\bar{r},j}$, $\breve{a}^{ps}_{1\bar{r},j}$, $\underline{p}^{ps}_{\bar{r},IF}$, $\underline{p}^{ps}_{\bar{r},GF}$ for $j = 1,2$ (cf. (19))
- Compute $\underline{\breve{\delta}}^{ps}_{,j}$ for $j = 1,2$ (cf. (18))

End

Output
- Array-aided SD-SPB corrections $\underline{\breve{\delta}}^{ps}_{,j}$ $(j = 1,2)$

Figure 3. Algorithmic steps in computing the array-aided SD-SPBs of satellite s, given the pivot satellite p.

NUMERICAL RESULTS

Experiment description

In this section, the methodology discussed above is evaluated by an array-based experiment organized by Curtin University in Perth, Australia. Table 1 presents the information on the collected data. Two GPS dual-frequency data-sets have been collected by 5 Javad receivers of the same type: 1) the array data-set of 4 antennas and 2) the user data-set of 1 antenna. The structure of the array and user has been visualized in Fig. 4. The array was located in Foreshore, South Perth, whereas the user station was set up at Bentley campus of Curtin University. The distance between the reference antenna of the array and the user antenna is about 4 [km]. All the data have been measured above a cut-off elevation of 10° with a sampling interval of 30 seconds. The array data-set is aimed to determine the SD-SPB corrections, while the user data-set is aimed to show the applicability of the stated corrections.

SD-SPB's precision improvement

We first consider the results of the array data-set. To gain some insight into the dependency of the SD-SPBs' preci-

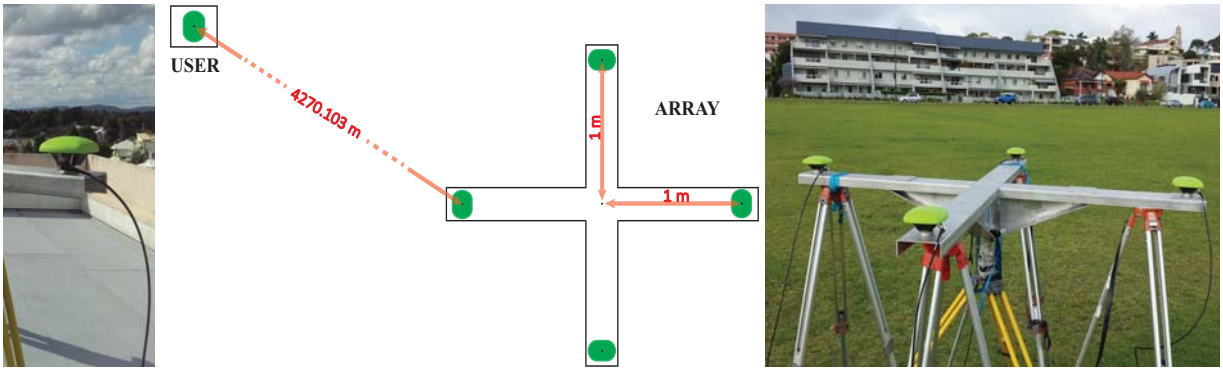

Figure 4. Structure of the user (left) and the array of antennas (right) as used in the experiment. The array is composed of four 1-meter arms. The distance between the user's antenna and the reference antenna of the array is about 4270 meters.

sion on the number of antennas, time-series of the single-epoch SD-SPB estimator have been presented. It is clear that the size of the fluctuations of each time-series gives an impression of the noise of the corresponding SD-SPB corrections. Shown in Fig. 5 are the time-series of the SD-SPB corrections as a function of the number of antennas. The results correspond to PRN23, given PRN13 as the pivot satellite. The noise reduction can be observed as the number of antennas increases from $n = 1$ (red line) to $n = 4$ (green line). This is the case with both the SD-SPBs on L1 and on L1-L2.

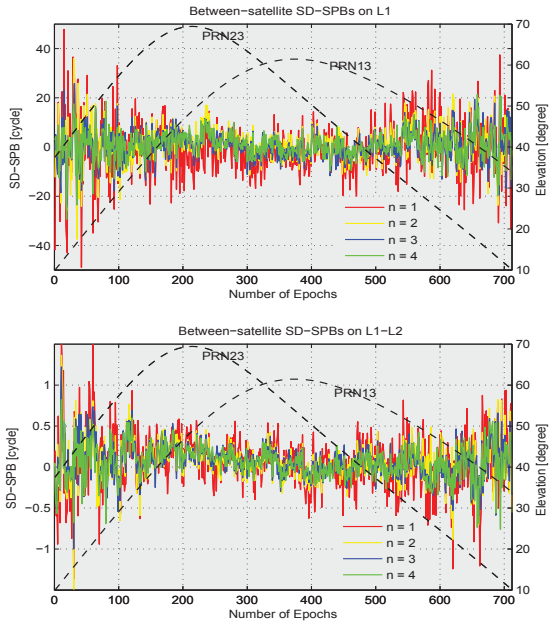

Figure 5. Single-epoch SD-SPB corrections on L1 (*top*) and on L1-L2 (*bottom*) over time as a function of the number of antennas (n). The results correspond to PRN23, given PRN13 as the pivot satellite. Satellites' elevation is depicted in black dashed line.

To quantify the noise of the single-epoch SD-SPB corrections, we make use of the root mean squared error (RMSE) of the time-series. The RMSE of the single-epoch array-aided SD-SPBs are given in Table 2. As shown, the RMSE of the single-antenna SD-SPBs on L1 is computed as 10.89 [cycle] which is almost 32 times larger than that of the SD-SPBs on L1-L2 (0.34 [cycle]). This is in agreement with the theoretical value already inferred from (12) and (13). According to (20), one would expect the ratio of the RMSE of the array-aided SD-SPBs to that of the single-antenna SD-SPBs to be approximated by $(1/\sqrt{n})$. The RMSE ratios have been compared to their theoretical counterparts in Table 2. As shown, the RMSE ratios and the theoretical values do interestingly coincide. In particular, we highlight that the RMSE of the single-epoch SD-SPBs on L1 decreases from 10.89 [cycle] to almost half its value, i.e. 5.52 [cycle].

A similar analysis has been carried out for other pairs of satellites. The results of the analysis are summarized in Fig. 6. The theoretical value $(1/\sqrt{n})$, depicted in green line, serves as reference. As illustrated, the RMSE ratios follow the reference trend dictated by the theoretical value.

Table 2. RMSE of the single-epoch SD-SPB corrections corresponding to PRN13 and PRN23 for different number of antennas. The RMSE ratio has been compared to its theoretical value $(1/\sqrt{n})$.

No. of antennas	$n = 1$		$n = 2$		$n = 3$		$n = 4$	
	L1	L1-L2	L1	L1-L2	L1	L1-L2	L1	L1-L2
RMSE [cycle]	10.89	0.34	7.74	0.23	6.34	0.20	5.52	0.18
RMSE ratio	1.00	1.00	0.71	0.68	0.58	0.59	0.51	0.53
Theoretical value	1.00	1.00	0.71	0.71	0.58	0.58	0.50	0.50

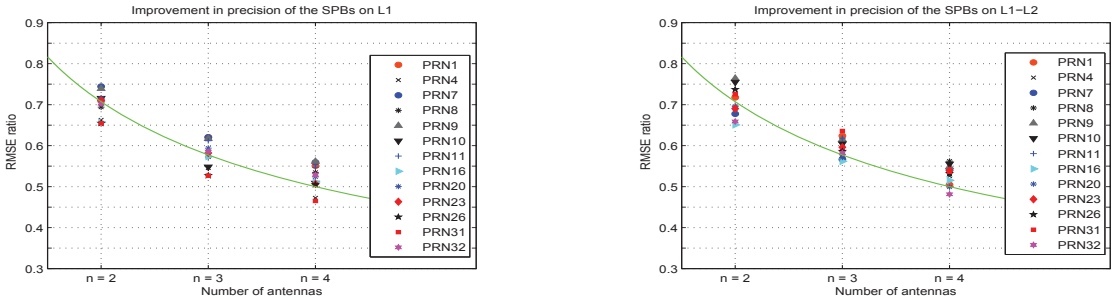

Figure 6. RMSE ratio of the array-aided SD-SPB corrections on L1 (left) and on L1-L2 (right), compared to the theoretical value $(1/\sqrt{n})$ (green line). PRN13 has been taken as the pivot satellite.

Integer recovery of the user's ambiguities

We now turn our attention to the results of the user data-set. Forming the between-satellite SD combinations of the user's observations, the receiver-specific unknown parameters are removed. Like the array data-set, the satellite positions have been computed using the orbits of the IGS. The estimable between-satellite SD satellite clocks and ionospheric delays have been estimated using the array data-set and sent to the user according to the strategy as described in [16, 18]. Since the distance between the array and the user is about 4 [km], correcting the user's data by the same ionospheric delays, estimated at the array's location, is realistically allowed. Corrected by the array-derived satellite clocks and ionospheric delays, the SD observation equations of the user only include the position and real-valued SD ambiguities as unknowns.

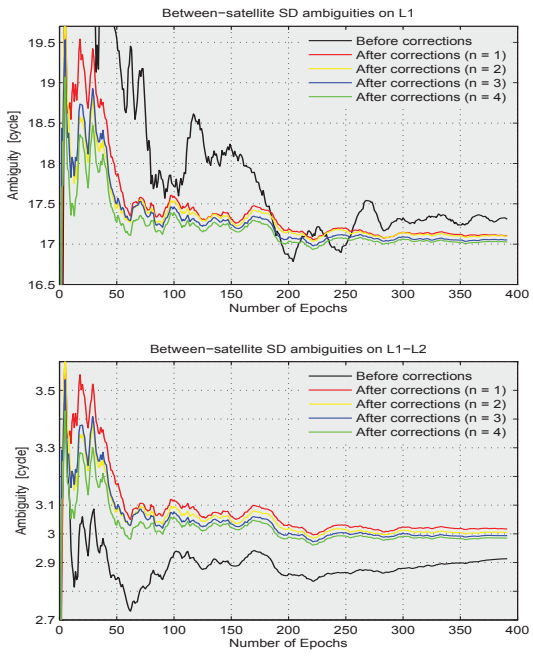

Figure 7. Convergence of the user's SD ambiguities on L1 (*top*) and on L1-L2 (*bottom*) over time. The results correspond to PRN32, given PRN13 as the pivot satellite.

We now evaluate the integer recovery role of the SD-SPB corrections. To do so, we consider the convergence of the user's SD ambiguities over time, once without applying the SD-SPB corrections, and another time with applying the SD-SPB corrections. The corresponding results have been illustrated in Fig. 7. It is clearly visible that the SD ambiguities, without corrections, do not tend to integer values. Corrected by the SD-SPBs however, the integer property of the SD ambiguities is recovered and they do indeed converge to integer values.

In view of the SD-SPBs' precision improvement discussed earlier, one would expect that the array-aided SD-SPBs expedite the ambiguities' convergence compared to the single-antenna SD-SPBs. This has been realized in Fig. 7. For instance, the minimum number of epochs after which the user's SD ambiguities on L1 never exceed half a cycle beyond the integer 17 is computed as $k = 118$ (for $n = 1$). This minimum number of epochs deceases to $k = 103$ (for $n = 2$), $k = 72$ (for $n = 3$), and $k = 44$ (for $n = 4$).

To see the improvement on the estimated user's position, the array-derived ionospheric corrections have been estimated and sent to the user, once based on the data of the reference antenna (i.e. $n = 1$), and another time based on the inclusion of the data of the other antennas (i.e. $n = 2,3,4$). The integer-recovered ambiguities have been then fixed epoch-by-epoch using the LAMBDA method [26]. Fig. 8 shows the North-East scatter of the estimated user's position before ambiguity-fixing (float case) and after ambiguity-fixing (fixed case). The results are accompanied by their corresponding 95% confidence ellipses. In both the float and fixed cases, the improvement occurs by switching from the single-antenna corrections ($n = 1$) to the array-aided corrections ($n = 4$). This is in agreement with the concept of *array-aided precise*

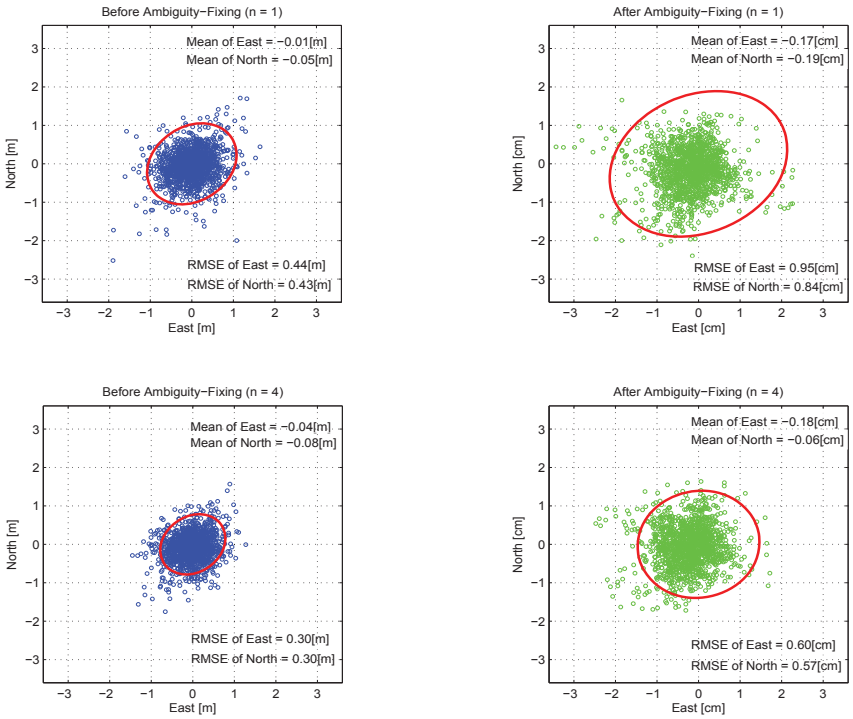

Figure 8. *Top-panel*: North-East position scatter of the user before (left) and after (right) ambiguity-fixing, on the basis of the single-antenna corrections ($n = 1$). *Bottom-panel*: North-East position scatter of the user before (left) and after (right) ambiguity-fixing, on the basis of the array-aided corrections ($n = 4$). The corresponding 95% confidence ellipses are depicted in red lines.

point positioning (A-PPP) which is originally introduced by [20]. In a more quantitative way, Table 3 presents the RMSE of the user's position components as a function of the number of antennas aiding the ionospheric and SD-SPB corrections.

We also remark that the significant improvement in the position upon ambiguity-fixing is due to the high precision of the phase observations which contribute to the model once the integer-recovered ambiguities are successfully resolved. This again confirms the applicability of the array-aided SPBs in recovering the integer property of the user's ambiguities

Table 3. RMSE of the user's position before ambiguity-fixing (*Float*: in centimeters) and after ambiguity-fixing (*Fixed*: in millimeters) based on the array-aided corrections of different number of antennas.

No. of antennas	$n = 1$		$n = 2$		$n = 3$		$n = 4$	
	Float	Fixed	Float	Fixed	Float	Fixed	Float	Fixed
RMSE of East	43.6	9.5	40.2	9.3	34.5	7.6	30.2	6.0
RMSE of North	43.4	8.4	39.2	7.9	34.4	7.1	29.8	5.7
RMSE of UP	98.1	21.2	89.3	19.3	86.7	16.1	83.9	14.0

SUMMARY AND CONCLUSIONS

In this contribution, we introduced the concept of array-aided between-satellite SD-SPBs determination. The underlying model is characterized by data of an array of GNSS antennas, mounted on rigid platforms, that are separated by short distances so that the same ionospheric delay is assumed to be experienced by all the antennas. Forming a full-rank GNSS model, the estimable SD-SPBs were shown to appear, for instance, as a combination of the true SD-SPBs, the SD satellite code hardware delays, and the SD ambiguities of a reference antenna. A closed-form expression of the array-aided SD-SPB corrections was presented through which a simple strategy to compute the SD-SPBs was outlined.

The closed-form expression of the SD-SPB estimator allows us to study the precision of the SD-SPB corrections analytically. In case of GPS dual-frequency data, the high positive correlation between the non-combined SD-SPBs on L1 and on L2 was quantified (about 0.9996), thus highlighting the existence of more precise combined SD-SPBs. It was shown that the standard deviation of the wide-lane SD-SPBs (on L1-L2) is expected to be almost 32 times smaller than that of their non-combined counter-

parts. Moreover, the cross-correlation between the wide-lane SD-SPBs and those on L1 is expected to be about 0.2581.

In order to reduce the code-dominated variance of the SD-SPB corrections, the data of extra antennas are incorporated into the model. As shown, the extra antennas give additional information on the SD-SPBs at the expense of additional unknowns, i.e. the array's DD ambiguities. After resolving the DD ambiguities of the array's data, the extra antennas do contribute to the precision of the SD-SPBs. With n being the number of all contributing antennas, the variance of the array-aided SD-SPB corrections is n times smaller than that of the single-antenna SD-SPB corrections. This precision improvement was also demonstrated by numerical results. As a consequence of which, the integer-recovered ambiguities of the user converge to integer values faster, upon increasing the number of aiding antennas. As a typical example, it was shown that the minimum number of epochs, say k, after which the user's SD ambiguities on L1 never exceed half a cycle beyond an integer was decreased from $k = 118$ (for $n = 1$) to $k = 44$ (for $n = 4$). The precision improvement can also be carried over to the user's position, would the array-aided SD-SPB corrections be accompanied by the ionospheric corrections.

ACKNOWLEDGEMENTS

The array-based experiment was conducted by Dr. N. Raziq and Dr. B. Padovan from Curtin University, Perth, Australia. This support is gratefully acknowledged.

REFERENCES

[1] P. Heroux and J. Kouba, "GPS precise point positioning with a difference," in *Paper presented at Geomatics 95, Ottawa, Canada*, pages 13–15, 1995.

[2] J. F. Zumberge, M. B. Heflin, D. C. Jefferson, M. M. Watkins, and F. H. Webb, "Precise point positioning for the efficient and robust analysis of GPS data from large networks," *J. Geophys. Res.*, vol. 102, pages 5005–5017, 1997.

[3] R. F. Leandro, M. C. Santos, and R. B. Langley, "Analyzing GNSS data in precise point positioning software," *GPS Solut.*, vol. 15, no. 1, pages 1–13, 2011.

[4] R. J. van Bree and C. C. Tiberius, "Real-time single-frequency precise point positioning: accuracy assessment," *GPS Solut.*, vol. 16, no. 2, pages 259–266, 2012.

[5] M. J. Gabor and R. S. Nerem, "Satellite-satellite single-difference phase bias calibration as applied to ambiguity resolution," *Navigation*, vol. 49, no. 4, pages 223–242, 2002.

[6] M. Ge, G. Gendt, M. Rothacher, C. Shi, and J. Liu, "Resolution of GPS carrier-phase ambiguities in precise point positioning (PPP) with daily observations," *J. Geod.*, vol. 82, no. 7, pages 389–399, 2008.

[7] D. Laurichesse, F. Mercier, J. Berthias, P. Broca, L. Cerri, and F. CNES, "Integer ambiguity resolution on undifferenced GPS phase measurements and its application to PPP and satellite precise orbit determination," *Navigation*, vol. 56, no. 2, pages 135–149, 2009.

[8] P. Collins, S. Bisnath, F. Lahaye, and P. Heroux, "Undifferenced GPS ambiguity resolution using the decoupled clock model and ambiguity datum fixing," *Navigation*, vol. 57, no. 2, pages 123–135, 2010.

[9] P. J. G. Teunissen, D. Odijk, and B. Zhang, "PPP-RTK: Results of CORS Network-Based PPP with Integer Ambiguity Resolution," *J. Aeronaut. Astronaut. Aviat.*, vol. 42, no. 4, pages 223–229, 2010.

[10] P. Henkel, Z. Wen, and C. Gunther, "Estimation of satellite and receiver biases on multiple Galileo frequencies with a Kalman filter," in *ION Proceedings of the 2010 International Technical Meeting of The Institute of Navigation, CA*, pages 1067–1074, 2010.

[11] S. Bisnath and P. Collins, "Recent developments in precise point positioning," *Geomatica*, vol. 66, no. 2, pages 103–111, 2012.

[12] J. Geng, C. Shi, M. Ge, A. H. Dodson, Y. Lou, Q. Zhao, and J. Liu, "Improving the estimation of fractional-cycle biases for ambiguity resolution in precise point positioning," *J. Geod.*, vol. 86, no. 8, pages 579–589, 2012.

[13] S. Loyer, F. Perosanz, F. Mercier, H. Capdeville, and J.-C. Marty, "Zero-difference GPS ambiguity resolution at CNES–CLS IGS Analysis Center," *J. Geod.*, vol. 86, no. 11, pages 991–1003, 2012.

[14] Z. Wen, P. Henkel, and C. Gunther, "Reliable estimation of phase biases of GPS satellites with a local reference network," in *ELMAR, 2011 Proceedings, Croatia*, pages 321–324, IEEE, 2011.

[15] X. Li and X. Zhang, "Improving the estimation of uncalibrated fractional phase offsets for PPP ambiguity resolution," *J. Navig.*, vol. 65, no. 03, pages 513–529, 2012.

[16] D. Odijk, P. J. G. Teunissen, and B. Zhang, "Single-frequency integer ambiguity resolution enabled GPS precise point positioning," *J. Surv. Eng.*, vol. 138, no. 4, pages 193–202, 2012.

[17] X. Zhang, P. Li, and F. Guo, "Ambiguity resolution in precise point positioning with hourly data for global single receiver," *Adv. Space Res.*, vol. 51, no. 1, pages 153 – 161, 2013.

[18] D. Odijk, P. J. G. Teunissen, and A. Khodabandeh, "Single-Frequency PPP-RTK: Theory and Experimental Results," *IAG Symp*, vol. 139, pages 167–173, 2014.

[19] X. Li, X. Zhang, and M. Ge, "Regional reference network augmented precise point positioning for instantaneous ambiguity resolution," *J. Geod.*, vol. 85, no. 3, pages 151–158, 2011.

[20] P. J. G. Teunissen, "A-PPP: Array-aided Precise Point Positioning with Global Navigation Satellite Systems," *IEEE Trans. Signal Process*, vol. 60, no. 6, pages 2870–2881, 2012.

[21] A. Khodabandeh and P. J. G. Teunissen, "Single-Epoch GNSS Array Integrity: an Analytical Study," *IAG Symp*, vol. 142, 2015. In press.

[22] B. Hofmann-Wellenhof, H. Lichtenegger, and E. Wasle, *GNSS: Global Navigation Satellite Systems: GPS, Glonass, Galileo, and More*. Springer, New York, 2008.

[23] P. J. G. Teunissen, "Generalized inverses, adjustment, the datum problem and S-transformations," in *Optimization and Design of Geodetic Networks* (E. W. Grafarend and F. Sanso, eds.), pages 11–55, Springer, Berlin, 1985.

[24] P. J. de Jonge, *A processing strategy for the application of the GPS in networks*. PhD thesis, Delft University of Technology, Publication on Geodesy, 46, Netherlands Geodetic Commission, Delft, 1998.

[25] H. J. Euler and C. C. Goad, "On optimal filtering of GPS dual frequency observations without using orbit information," *J. Geod.*, vol. 65, no. 2, pages 130–143, 1991.

[26] P. J. G. Teunissen, "The least-squares ambiguity decorrelation adjustment: a method for fast GPS integer ambiguity estimation," *J. Geod.*, vol. 70, no. 1-2, pages 65–82, 1995.